wjert, 2020, Vol. 6, Issue 5, 438-462. Research Article ISSN 2454-695X

World Journal of Engineering Research and Technology

WJERT

www.wjert.org

SJIF Impact Factor: 5.924

SWITCHED-CAPACITOR/SWITCHED-INDUCTOR STRUCTURES FOR GETTING TRANSFORMERLESS BIDIRECTIONAL DC–DC PWM CONVERTERS: STEADY STATE AND DYNAMICS

Boris Axelrod, Yefim Berkovich* and Sagi Moshe

Department of Electrical Engineering, Holon Institute of Technology, 52 Golomb st., Holon, 58102, Israel.

Article Received on 20/08/2020 **Article Revised on 09/09/2020** **Article Accepted on 30/09/2020**

***Corresponding Author**
Dr. Yefim Berkovich
Department of Electrical Engineering, Holon Institute of Technology, 52 Golomb st., Holon, 58102, Israel.

ABSTRACT

This paper is devoted to expanding sphere of application of the universal Switched-Capacitor/ Switched-Inductor Structures by replacing the diodes with MOSFETs. These structures allow to build a large family of bidirectional converters with an increased/decreased voltage ratio depending on the operating mode. These structures are based on the three diode blocks proposed for decrease the voltage and three diode blocks for increase it. The use of MOSFETs allow to save all the properties of these structures in the diode mode, but also to obtain new possibilities when the transistors operate themselves. At the same time, the step-down structures become increasing, and, conversely, the step-up structures become decreasing. The paper describes the basic structures, describes the Boost / Buck and Buck-Boost bidirectional converters, and shows opportunity of their use in bidirectional Cuk, Sepic and Zeta converters. To analyze the dynamics of such converters having a rather complicated structure, a methodology for replacing them with an equivalent circuit of a conventional converter of the same type, the dynamic characteristics of which are well known, is proposed. An analysis of their work and the results of the experiment are given, which confirm the correctness of the conclusions.

KEYWORDS: Switched-Capacitor/ Switched-Inductor Structures, High Voltage Gain, DC-DC Bidirectional Converters, Dynamics.

1. INTRODUCTION

One of the main areas in improving DC-DC converters is the problem of expanding of the output voltage regulation range (Ioinovici, 2013). For converters that increase the output voltage, in particular boost converter, this requirement is expressed in a significant increase in the output voltage gain, while for step-down converters, for example, in buck converter, the output voltage should be as low as possible.

The main technical means for achieving these goals can be divided into the following areas: cascade connections converters, magnetically coupled inductors, diode-capacitor multipliers (dividers) of voltage and structures with switched capacitors (SC) or switched inductors (SL). Separately, can be mention the methods based on a combination of all these main areas. The idea of cascade connection converters is presented in (Maksimovic´, et al., 1991), and magnetically coupled inductors - in (Zhao, et al., 2001, 2003, Axelrod, et al., 2006). An additional development of the idea of magnetically coupled inductors was provided in (Wai, et al., 2005, 2007, Axelrod, et al., 2009), which indicated the possibility of an additional increase in the output voltage gain and a decrease of the stress on the switches and diodes. Of particular note is the proposal of a negative coupling coefficient – (Li, et al., 2018, Gao, et al., 2018), which makes it possible to increase the output voltage while reducing the ratio of coils of magnetically coupled inductors.

Another effective means of significantly increasing the output voltage gain in boost converters is the voltage multipliers Cockroft-Walton and Dickson (Feng, et al., 2006). In earlier publications on this subject, these multipliers were connected in parallel to the boost converter switch for unidirectional voltage – (Ganesan, et al., 2013, Axelrod, et al., 2012). In subsequent publications, such multipliers were proposed to be connected to a bidirectional voltage, which led to an even higher voltage gain and reduction of losses in the converter (Kim, et al., 2011, Ganesan, et al., 2014, Young, et al., 2013]. Of interest are schemes for connecting multipliers to voltage with two frequencies, for example, (Prince, et al., 2013).

In addition to the main directions listed above, the so-called switched capacitors converters are also developing. These converters contain only capacitors, switches and diodes - without inductors and they have found use at low powers (Ioinovici, 2001), since they contain, as a rule, a large number of switches and other elements. The possibility of using switched capacitors in conventional boost converters without additional switches is shown in (Axelrod, et al., 2003), then in (Axelrod, et al., 2004, 2004, 2006). In (Axelrod, et al., 2008), this

proposal was also generalized to switched inductors (SL) and the use of various modifications of typical structures of switched capacitors and switched inductors on diodes was shown to both reduce and increase voltage in converters of various types (see also (Axelrod, et al., 2009)). Generalized modifications of other SC-SL structures and various schemes of their connections are described in (Li, et al., 2016). Detailed reviews (Forouzesh, et al., 2017, De Paula, et al., 2014, Sivakumar, et al., 2017, Amir, et al., 2018) describe various combinations of switching on SC and SL structures (modules) and many possible modifications of converters based on a combination of the basic solutions described in (Axelrod, et al., 2008).

Among the general technical solutions aimed at improving the DC-DC converters, it is also can be noting solutions based on a combination of the above main directions - magnetically coupled inductors together with a voltage multiplier or with SC and SL structures (Baek, et al., 2005, Liang, et al., 2012, Axelrod, et al., 2015], as well as solutions, based on the use of various modifications of Luo-converters (Luo, 2011).

The attractive side of the structures (Axelrod, et al., 2008) was that the switching in them was carried out using diodes without additional controlled switches and, accordingly, without additional control channels. At the same time, in the regard with the wide development of systems with renewable energy sources and also with the development of electric transport, DC-DC bidirectional converters have become great relevance, providing an increase in voltage in one direction of energy transfer and a decrease in voltage in the other (Li-Jun, et al., 2015, Pathak, et al., 2015,).

It is known that renewable energy sources are characterized by variable output power. Therefore, they are combined with energy storage devices using bidirectional converters. If there is an excess of energy, they send part of it, for example, to the battery, using the step-down mode of the converter. When there is a lack of energy, it is directed back from the storage device to the load using a step-up mode. Another application of bidirectional converters is in electric drive systems, - modes of power supply and regulation of the motor when the voltage rises and braking modes - when it is lowered.

These converters also need to expand the control range using, in particular, SC and SL modules. Separate modifications of such converters are presented in (Cornea, et al., 2017) and (Axelrod, et al., 2019). It is quite obvious that, like all other active elements in

bidirectional converters, diodes in SC and SL modules must also be replaced with bidirectional switches (for example, MOSFETs). This paper, which is an extension of (Axelrod, et al., 2008), presents modifications of SC and SL modules on bidirectional switches and their application in all types of classic DC-DC converters. All the proposed structures are also applicable in the converters of Cuk, Sepic and Zeta. The corresponding circuits for diodes are shown in (Axelrod, et al., 2008).

It must be emphasized that all the above described directions to ensure the expansion of the output voltage regulation range in the converters inevitably lead to the complexity of their circuits and to an increase in the number of active and reactive elements. This leads to the complication or even the practical impossibility of a theoretical analysis of the dynamic modes of these converters by known linearization methods (Middlebrook, et al., 1976).

Therefore, the presented paper proposes a new approach to analyzing the dynamics of such circuits using converters with SC and SL structures as an example. The method is based on linearization on the basis of energy balance and allows you to replace the original complicated converter with its conventional form, but with modified parameters, however with the same dynamic characteristics, which are also well studied.

The paper consists of two parts. The first part describes the proposed schemes of new converters and their static characteristics, and the second gives an analysis of their dynamic modes. The first part consists of three sections - Section II, III and IV, while Section II describes the twelve basic structures of SC and SL modules, Section III presents hybrid bidirectional Boost / Buck converter, and in a Section IV - new bidirectional DC – DC converters based on Buck-Boost converters.

The second part consists of three sections - V-VII. The first of them gives an introduction to the proposed linearization method and analysis of two types of hybrid bidirectional Boost / Buck converter - one based on the SC structure, and the other based on the SL structure. Section VI on the same converters shows a technique for generating equivalent conventional converters. Section VII is devoted to the results of experimental verification of dynamic modes in the indicated converters.

2. Switched-Capacitor/Switched-Inductor Step-Down/ Step-Up Structures

Earlier, in (Axelrod, et al., 2008), three structures with the use of diodes were proposed. These structures provide decrease of the output voltage in DC-DC PWM converters with an improved conversion ratio. They were denoted by Dn1, Dn2, Dn3 ("Dn" – means Down). These structures, obviously, save the ability to work as diodes when replacing the diodes with MOSFETs - in the absence of control pulses on the transistors. Now they will be denoted Dn1D, Dn2D, Dn3D (D - diode). When transistors are operate (as controlled switches), these same structures acquire the possibility, on the contrary, to increase the output voltage.

Corresponding structures will be denoted Up1S, Up2S, Up3S - the designation reflects the increase in voltage and the operation of the S switch. Fig. 1a shows three pair of corresponding configurations Dn1D-Up1S; Dn2D-Up2S; Dn3D-Up3S. The transistors and diodes operating in each configuration are reflected in thick lines.

A similar situation with the previously proposed step-up structures - now in their designation will appear the sign "D", i.e. the diodes operate, and in the reverse mode – sign "S", i.e. transistors operate. Fig. 1b shows three pairs of corresponding configurations Up1D-Dn1S; Up2D-Dn2S; Up3D-Dn3S;

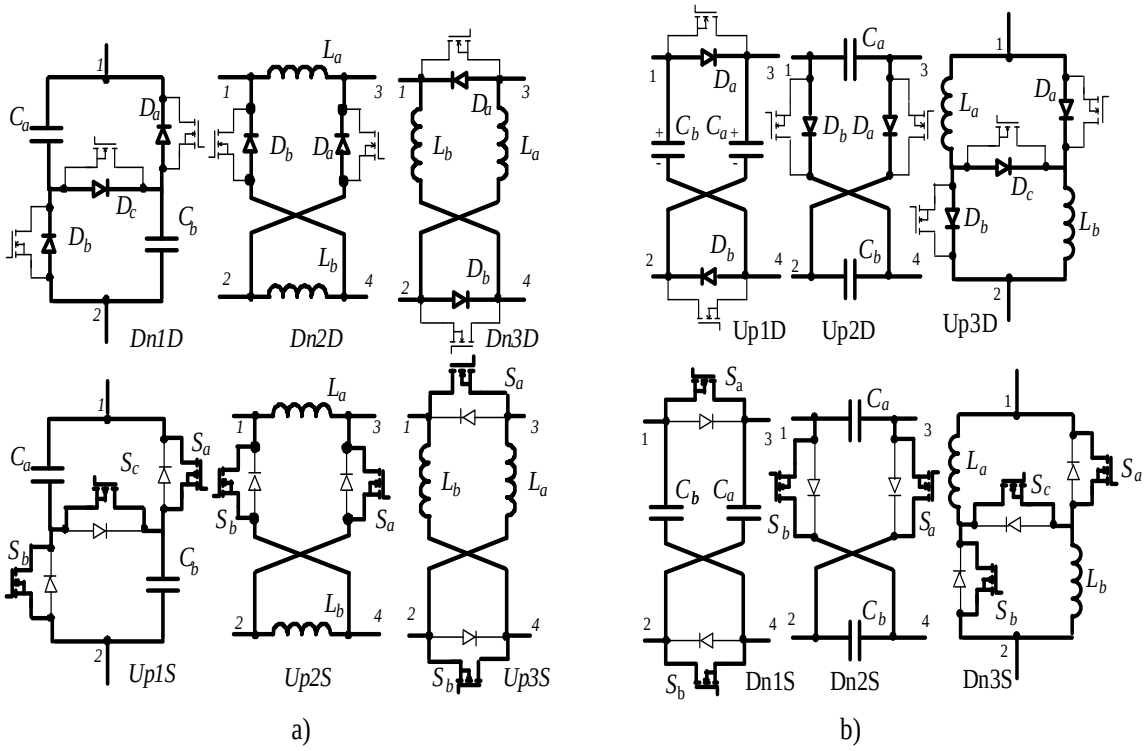

Fig. 1: Basic switching blocks, a) Step-down/step-up blocks.

b) Step-up/step-down blocks

3. New Basic Hybrid Bidirectional Boost/Buck Converters

Let us begin the description of various circuits of bidirectional converters from the most common case, when voltage is converted from left to right (boost mode), and from right to left (buck mode). The common name of such a converter will be Boost / Buck converter, its possible modifications are shown in Fig. 2. Note that the modifications of Boost/Buck converters with the Up2D-Dn2S and Dn3D-Up3S blocks coincide with the modifications of Fig. 2b and Fig. 2c respectively. But in this case, the output voltage V_2 reverses its sign.

Table 1 presents all the possible combinations of the above structures in various circuits of bidirectional DC-DC converters. Consider these options.

The operation of the presented structures becomes clear if we write the operation of switches and diodes for each of them both in the voltage increase mode (energy direction from left to right) and in the voltage decrease mode (energy direction from right to left).

Table 2a corresponds to the modification presented in Fig. 2a and so on (Tables 2b, 2c, 2d). In all these tables, "1" indicates the conductive state of the element, and "0" - non-conductive state. Functioning areas of the switches or diodes in different structures are

Table 1: Possible realizations of bidirectional converters with *C-/L*-Switching Structures.

C-/L-Switching Structures / Converters	Dn1D-Up1S	Dn2D-Up2S	Dn3D-Up3S	Up1D-Dn1S	Up2D-Dn2S	Up3D-Dn3S
Buck/Boost	⊗	⊗	⊗[1]	⊗	⊗[1]	⊗
Buck-Boost	⊗	⊗[2]	⊗	⊗	⊗[2]	⊗

[1] - Inverting Buck/Boost;

[2] - Non- inverting Buck-Boost.

marked into frames. The designations *S1* and *S2* reflect the ability of the device to function in the switch mode (S) or in the diode mode (D).

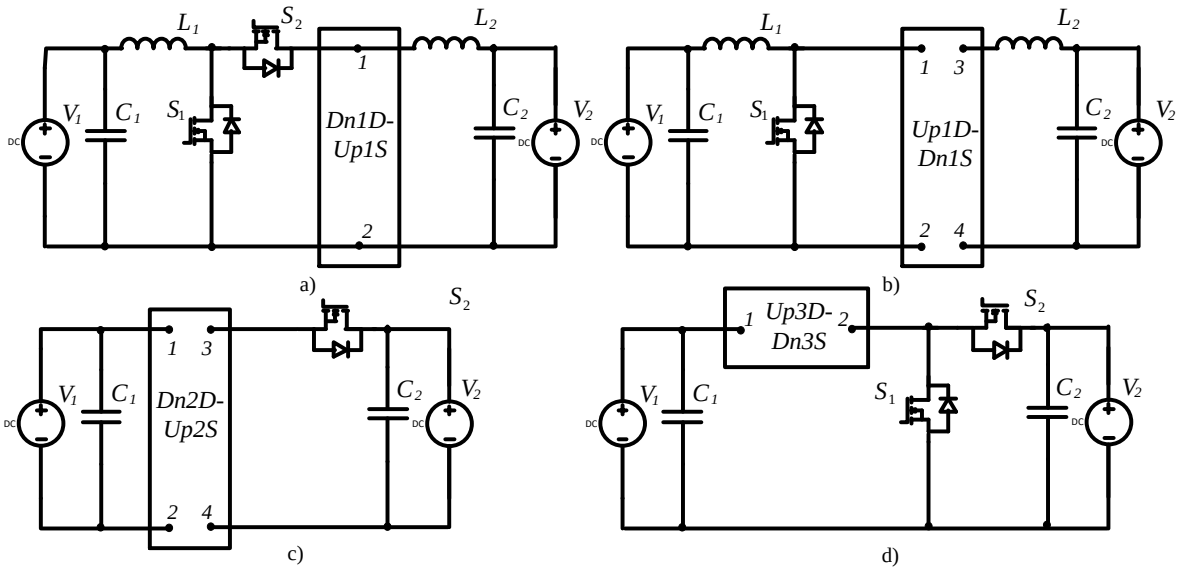

Fig. 2: Modifications of the Boost/Buck converter with step-down and step-up structures.

Table 2a: Operation of the switches and diodes in both direction of energy for the modification of Fig. 2a.

Regimes of Converters Fig. 2a		**S1**		**S2**		**Dn1D**		**Up1S**	
		S	**D**	**S**	**D**	**Da Db**	**Dc**	**Sa Sb**	**Sc**
Boost	ton	1	0	0	0	0	0	0	1
	toff	0	0	0	1	0	0	1	0
Buck	ton	0	0	1	0	1	0	0	0
	toff	0	1	0	0	0	1	0	0

Table 2b: Operation of the switches and diodes in both direction of energy for the modification of Fig. 2b.

Regimes of Converter Fig. 2b		**S1**		**Dn1S Dn2S**		**Up1D Up2D**	
		S	**D**	**Sa**	**Sb**	**Da**	**Db**
Boost	ton	1	0	0	0	0	0
	toff	0	0	0	0	1	1
Buck	ton	0	0	1	1	0	0
	toff	0	1	0	0	0	0

Table 2c: Operation of the switches and diodes in both direction of energy for the modification of Fig. 2c.

Regimes of Converter Fig. 2c		S2		Dn2D Dn3D		Up2S Up3S	
		S	D	Da	Db	Sa	Sb
Boost	ton	0	0	0	0	1	1
	toff	0	1	0	0	0	0
Buck	ton	1	0	0	0	0	0
	toff	0	0	1	1	0	0

Table 2d: Operation of the switches and diodes in both direction of energy for the modification of Fig. 2d.

Regimes of Converter Fig. 2d		S1		S2		Up3D		Dn3S	
		S	D	S	D	Da, Db	Dc	Sa, Sb	Sc
Boost	ton	1	0	0	0	1	0	0	0
	toff	0	0	0	1	0	1	0	0
Buck	ton	0	0	1	0	0	0	0	1
	toff	0	1	0	0	0	0	1	0

Consider on the basis of Table. 2a the functioning of the switches in the converter Fig. 2a. In the boost converter mode, when the energy is directed from the left to the right source, at the interval t_{on} the switches *S1* and *Sc* in the block Up1S are turned on. Diode *D* of the converter is blocked. In this case, the voltage of two series-connected capacitors of the block Up1S will be applied to the load. At the interval t_{off}, these switches are turned off and two switches *Sa* and *Sb* of the block Up1S turn on. In this case, the capacitors of the block are connected in parallel, and the voltage across the load will be half. Thus, due to the double voltage on the interval t_{on}, the average value of the voltage across the load will be greater and equal to $V2 = V1\ (1 + D) / (1-D)$ (Axelrod, et al., 2008).

In the buck converter mode, during t_{off}, all switches are open, and the capacitors of the block Dn1D, connected in series through the diode *Dc*, are each charged to a voltage of $V2 / 2$. The inductor current of *L1* is closed through the diode of the transistor *S1*. At the interval t_{on}, switch *S2* is closed and the voltage of two parallel-connected capacitors with a voltage of $V2 / 2$ is applied to the load through the diodes *Da* and *Db*. As a result, the output voltage of the buck converter will be $V1 = V2D / (2-D)$ (Axelrod, et al., 2008).

If the duty cycle *D* of the switches S1 or S2 is designated in their conducting state, and also *D1 =1-D*, then the voltage ratio factors *M = Vo / Vin* for boost converter for all types of circuits can be written as

$$M_{boost} = \frac{1+D}{D1} \qquad (1)$$

and for the buck converter

$$M_{buck} = \frac{D}{1+D1} \qquad (2)$$

From (1) and (2), it can be seen that in the boost converter mode, the voltage is increased by *1 + D* times, which for large values of *D* approaches a double value. In buck converter mode, the voltage is reduced by *1+ D1* times, which, on the contrary, at small values of *D*, approaches a double value.

As indicated in the note to table 1, the structures Dn3D-Up3S and Up2D-Dn2S lead to a change in the sign of the output voltage, i.e., they are inverting.

4. New Hybrid Bidirectional Buck–Boost Converters

In this section, we describe the modifications of bidirectional converters, when the voltage conversion according to the scheme from left to right and the inverse conversion from right to left is carried out in the Buck-Boost converter mode. This will be the common name of such converters; their possible modifications are shown in Fig. 3.

The analysis shows that the tables of state of the switches and diodes in these modifications of bidirectional Boost-Buck converters completely coincide with the tables 2a-2d for the Boost / Buck modes. However, the values of the voltage ratio *M* for different structures are different. The corresponding expressions are presented in Table 3.

The table shows that in the boost mode, a double increase in the output voltage is provided (for the Dn1D-Up1S structure, it is *1 + D* times more - (a)). In the buck mode,

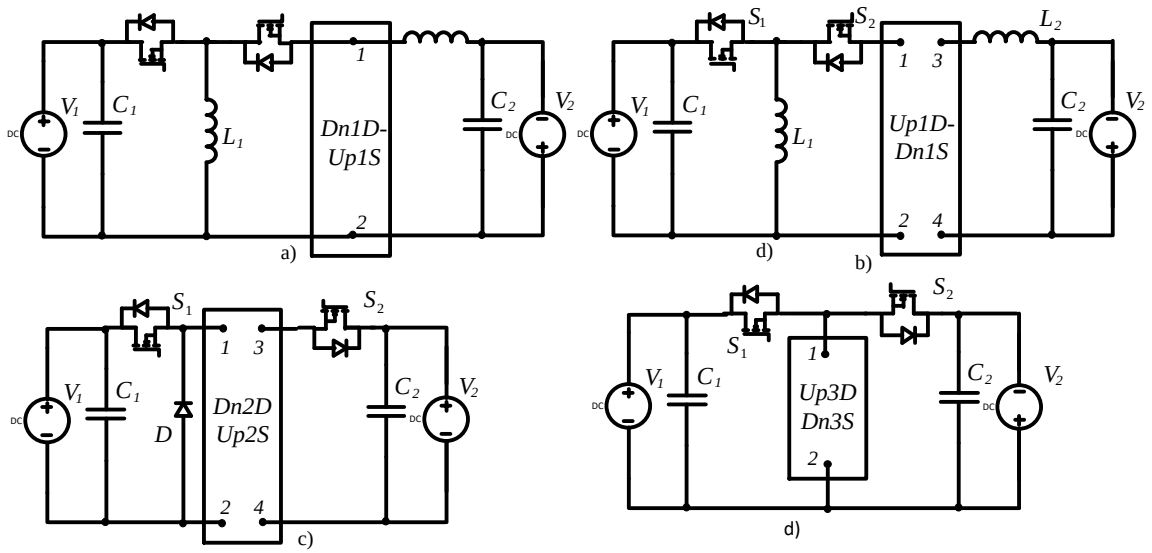

Fig. 3: Modifications of the Buck-Boost converters with step-down and step-up structures.

Expressions (h) and (l) show that the voltage decrease two times lower than in the conventional buck-boost converter. According to (b) and (d), the voltage decrease is (1 + D1) times smaller, which at small values of D approaches a double value. At the same time, the

Table 3: Voltage ratio in possible regimes of bidirectional buck-boost Converters with *C-/L*-switching structures.

C/L-Switching Structures	**Dn1D-Up1S**	**Up1D-Dn1S**	**Up2D-Dn2S**	**Up2D-Dn2S**	**Dn3D-Up3S**	**Up3D-Dn3S**
Regime Boost	$\frac{D(1+D)}{1-D}$ (a)	$\frac{2D}{1-D}$ (c)	$\frac{2D}{1-D}$ (e)	$\frac{2D}{1-D}$ (g)	$\frac{2D}{1-D}$ (i)	$\frac{2D}{1-D}$ (k)
Regime Buck	$\frac{D}{(1-D)(1+D1)}$ (b)	$\frac{D}{(1-D)(1+D1)}$ (d)	$\frac{D}{1+D1}$ (f)	$\frac{D}{2(1-D)}$ (h)	$\frac{D}{1+D1}$ (j)	$\frac{D}{2(1-D)}$ (l)

two structures - (h) and (l) operate as buck converter, but with a decrease in the output voltage *(1 + D1)* times more.

As indicated in the notes to table 1, the structures Dn2D-Up2S and Up2D-Dn2S lead to change in sign of the output voltage, that is, as for buck-boost converter, they lead to a non-inverting mode. When applying the Dn2D-Up2S and Dn3D-Up3S structures, the installation of an additional diode is required, without this diodes the converter turns into a boost converter.

Note that the modifications of Buck-boost converters with the Up2D-Dn2S and Dn3D-Up3S blocks coincide with the modifications of Fig. 3b and Fig. 3c respectively. But in this case, the output voltage V_2 reverses its sign.

5. Dynamic modes of the proposed converters. Introduction to the proposed linearization method

For the analysis of dynamic modes in DC converters, the well-known small signal analysis (SSA) method is used (Middlebrook, et al., 1976). However, the use of SSA to analyze the dynamics of the proposed schemes (in particular, Fig. 2a, Fig. 2b, Fig. 2d) requires the preparation and transformation of systems of fourth-order differential equations, which makes such an analysis difficult and its results are poorly observable. This paper proposes a simpler linearization method. It provides an equivalent linear circuit (usually of the second order) for each of the proposed converters. And further, the method assumes the analysis of an equivalent conventional boost or buck converter, the dynamic modes of which are identical to those in the original more complex converters. The method is based on the balance of energy increments in the basic and equivalent schemes and was partially presented in (Axelrod, et al., 2015).

Consider a simple boost converter (Fig. 4a), which is described by the following system of equations:

$$\begin{aligned} L\frac{di}{dt}+d_1(t)v&=v_{in} \\ C\frac{dv}{dt}+\frac{v}{R}&=d_1(t)i \end{aligned} \qquad (3)$$

Where $d_1(t)$) is the switching function, $d_1(t)=1-d(t)$ and $d(t)=1$ on the interval t_{on} and $d(t)=0$ on the interval t_{off}. Multiplying the first equation by i and the second by v ($i\neq 0,\ v\neq 0$) and summing the two obtained equations, we exclude the switching function:

$$Li\frac{di}{dt}+Cv\frac{dv}{dt}+\frac{v^2}{R}=v_{in}i \qquad (4)$$

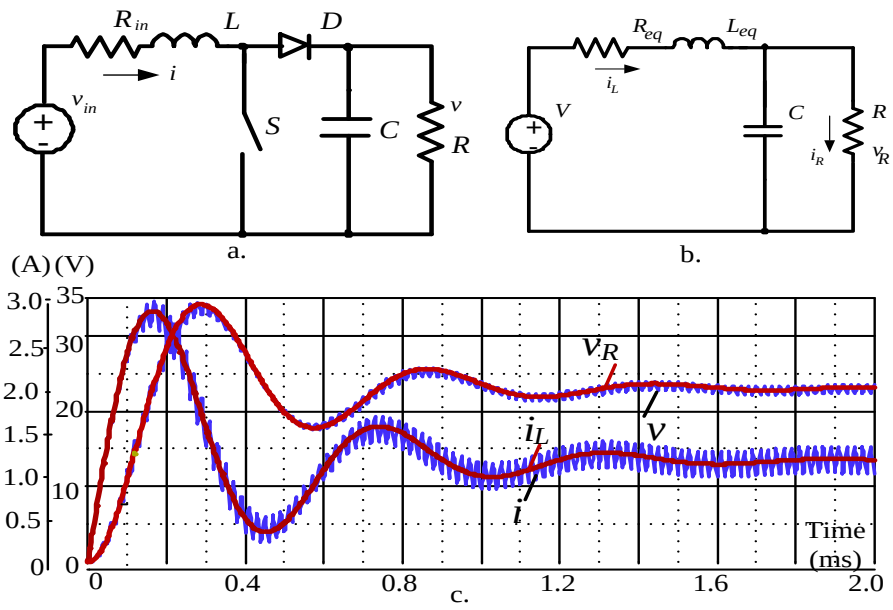

Fig. 4*:* Justification of the proposed linearization method (a) boost converter (b) the equivalent linear circuit (c) method validation in PSPICE.

After averaging the values i and v by integrating the equation during each period, i.e., going to their integral (average) values (indicated by the sign "tilde" - $\tilde{x} = \frac{1}{T}\int_t^{t+T} x dt$), we obtain the equation of energy increment balance

$$L\tilde{i}_{av}\Delta\tilde{i} + C\tilde{v}_{av}\Delta\tilde{v} + \frac{\tilde{v}^2}{R}T = v_{in}\tilde{i}_{av}T \qquad (5)$$

Here $\tilde{i}_{av} = (1/2)\left(\tilde{i}(t) + \tilde{i}(t+T)\right)$ and $\tilde{v}_{av} = (1/2)\left(\tilde{v}(t) + \tilde{v}(t+T)\right)$ are the average vales for each current averaged period of the values of current and voltage, $\Delta\tilde{i} = \tilde{i}(t+T) - \tilde{i}(t)$, $\Delta\tilde{v} = \tilde{v}(t+T) - \tilde{v}(t)$, are the changes of the averaged values of current and voltage during each period. We will further assume that at each period for the averaged values of the load current: $\tilde{i}_{R.av} = \tilde{i}_{av}D_1$ and load voltage $\tilde{v}_{av} = v_{in}/D_1$. We write the input current reduced to the output voltage $\tilde{i}_{L.av} = \tilde{i}_{av}D_1$ and $\Delta\tilde{i}_L = \Delta\tilde{i}D_1$ i.e., in the expression $L\tilde{i}_{av}\Delta\tilde{i}$ in (5) $\tilde{i}_{av} = \tilde{i}_{L.av}/D_1$ and $\Delta\tilde{i}_L = \Delta\tilde{i}D_1$. Now the last equation is written as

$$\frac{L}{D_1^2}\tilde{i}_{L.av}\Delta\tilde{i}_L + C\tilde{v}_{av}\Delta\tilde{v} + \frac{\tilde{v}_{av}^2}{R}T = \tilde{v}_{av}\tilde{i}_{R.av}T \qquad (6)$$

If v_{in} is a step function with a level V_{in}, then in the steady state we get $V = V_{in}/D_1$. The energy increment balance equation (5), compiled for the boost converter, corresponds to an

equivalent linear circuit $L_{eq}-(C\,||\,R)$, while $L_{eq}=L/D_1^2$ and the supply voltage is V (Fig. 4b).

This suggests that the transient in the obtained equivalent circuit corresponds to the transient in the boost converter considering the linearization. Note that in the linear model Fig. 4b should be included be active resistance R_{eq}. It consider losses in the boost converter and is reduce to the output circuit by multiplying by a factor $1/D_1^2$: $R_{eq}=R_{in}/D_1^2$.

To illustrate the effectiveness of the method in Fig. 4c shows the simulation results in the PSPICE program of the transient in the scheme with parameters: $V_{in}=12V$, $L=400\mu H$, $C=5\mu F$, $R=50\Omega$, $f=50kHz$, $D=0.5$.

Further, on the basis of the proposed approach, we will analyze the dynamics using of some example Fig. 2. In Fig. 5, they are presented in a simplified form - depending on the direction of energy conversion and, accordingly, the operation of diodes or transistors.

5-1. Boost converter with block Up1D. As the first example of applying this approach to the analysis of dynamic modes in the above-proposed converters, we will conduct such an analysis for the boost converter circuit with the block Up1D (Fig. 5a). If we accept $v_a = v_b = v_c$ and $C_a=C_b=C$, the system of equations in this case takes the form:

$$\begin{aligned}
&L_1\frac{di_1}{dt}+d_1(t)\cdot v_c=v_1\\
&L_2\frac{di_{L2}}{dt}-2v_c+d_1(t)\cdot v_c+v_2=0\\
&2d(t)\cdot C\frac{dv_c}{dt}+2d_1(t)\cdot C\frac{dv_c}{dt}+2d(t)\cdot i_{L2}+d_1(t)\cdot i_{L2}=d_1(t)\cdot i_1\\
&C_2\frac{dv_2}{dt}+\frac{v_2}{R_2}=i_{L2}
\end{aligned}\qquad(7)$$

Multiplying the first equation by i_1, and the third equation by v_c, after summing them and considering the second equation we get:

$$\begin{aligned}
&L_1 i_1\frac{di_1}{dt}+2d(t)\cdot v_c C\frac{dv_c}{dt}+2d_1(t)\cdot v_c C\frac{dv_c}{dt}+\\
&+i_{L2}(L_2\frac{di_{L2}}{dt}+v_2)=v_1\cdot i_1
\end{aligned}\qquad(8)$$

After averaging we get

$$L_1\tilde{i}_{1.av}\Delta\tilde{i}_1 + 2DC\tilde{v}_{c.av}\Delta\tilde{v}_c + 2D_1C\tilde{v}_{c.av}\Delta\tilde{v}_c + L_2\tilde{i}_{L2.av}\Delta\tilde{i}_{L2} + \tilde{i}_{L2.av}\tilde{v}_{2.av}T = v_1\tilde{i}_{1.av}T \quad (9)$$

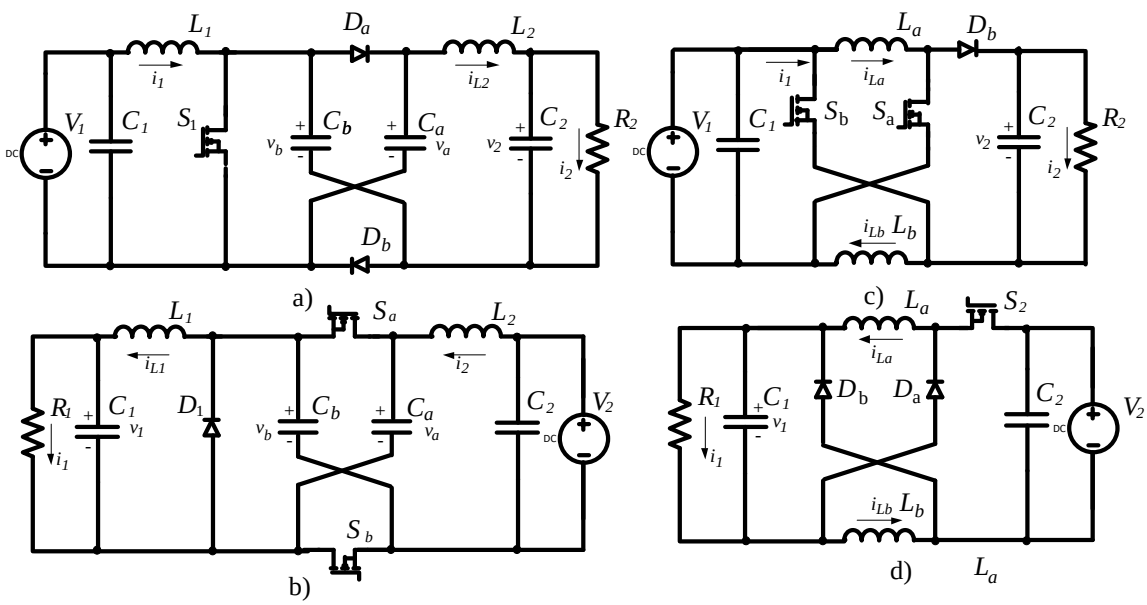

Fig. 5: Converter circuits with blocks (a) Up1D (b) Dn1S (c) Up2S (d) Dn2D.

Note that the transition to averaging the values of voltages and currents also makes it possible to replace the switching functions *d1(t)* and *d(t)* by their average values - respectively D1 and D. The transformations of the last equation give:

$$L_1M^2\tilde{i}_{1L}\Delta\tilde{i}_{1L} + 2D\frac{C}{M_1^2}\tilde{v}_{2.av}\Delta\tilde{v}_2 + 2D_1\frac{C}{M_1^2}\tilde{v}_{2.av}\Delta\tilde{v}_2 + L_2\tilde{i}_{L2.av}\Delta\tilde{i}_{L2} + \tilde{i}_{L2.av}\tilde{v}_{2.av}T = v_1\tilde{i}_{1.av}T \quad (10)$$

Here $M = (1+D)/(1-D)$, $M_1 = 1+D$, $\tilde{i}_{1L}$, $\Delta\tilde{i}_{1L}$ - the currents reduced to the output voltage, $\tilde{i}_{1.av} = \tilde{i}_{1L}M$, $\Delta\tilde{i}_1 = \Delta\tilde{i}_{1L}M$. Since $D + D_1 = 1$, the sum

$$2D\frac{C}{M_1^2}\tilde{v}_{2.av}\Delta\tilde{v}_2 + 2D_1\frac{C}{M_1^2}\tilde{v}_{2.av}\Delta\tilde{v}_2 = \frac{2C}{M_1^2}\tilde{v}_{2.av}\Delta\tilde{v}_2 \quad (11)$$

i.e., (10) is written as

$$L_1M^2\tilde{i}_{1L}\Delta\tilde{i}_{1L} + \frac{2C}{M_1^2}\tilde{v}_{2.av}\Delta\tilde{v}_2 + L_2\tilde{i}_{L2.av}\Delta\tilde{i}_{L2} + \tilde{i}_{L2.av}\tilde{v}_{2.av}T = \tilde{v}_{2.av}\tilde{i}_{2.av}T \quad (12)$$

The resulting expression may correspond to a linear circuit consisting of the input inductance $L_1M^2 = L_{eq}$, capacitor $2C/M_1^2 = C_{eq}$, inductance L_2, output capacitor C_2 and load R_2. Obviously, due to the equality of voltages, capacitor $2C/M_1^2 = C_{eq}$ can be

transferred to the right and combined with capacitor C_2. But at the same time inductance L_2 will be transferred to the left in the direction of a larger current, since its current now also includes the current of the capacitor C_{eq} ($i_{L2} > i_2$).To keep the energy of this inductance unchanged, it must be reduced by a factor of M_1^2, the same as the decrease of capacitors C.

As a result, we obtain the final equivalent circuit $L_{1.eq} \to L_{2.eq} \to C_{eq} \| C_2 \| R_2$, where $L_{1.eq} = L_1 M^2$, $L_{2.eq} = L_2 / M_1^2$, $C_{eq} = 2C / M_1^2$ at supply voltage $V_{in.eq} = V_{in} M$. Considering the connection of series inductances $L_{1.eq}$ and $L_{2.eq}$, and parallel-connected capacitors C_{eq} and C_2 the final equivalent circuit $(L_{1.eq} + L_{2.eq}) \to (C_{eq} + C_2) \| R_2$ with the structure Fig. 4b.

5-2. Buck converter with block Dn1S. Next, we analyze the circuit of Fig. 5b with a block Dn1S. The converter is powered in the opposite direction (Figs. 1b; 2b) - operate transistors *Sa*, *Sb*, instead of the diodes and instead of transistor *S1* operates a diode. The circuit generally function as a buck converter with a gain $M = D/(2-D)$. Assuming as before $v_a = v_b = v_c$ and C_a=C_b=C, compose a system of equations describing the operation of this circuit:

$$\begin{aligned}
&L_2 \frac{di_2}{dt} + d(t) \cdot v_c + d_1(t) 2 v_c = v_2 \\
&2d(t) \cdot C \frac{dv_c}{dt} + 2d_1(t) \cdot C \frac{dv_c}{dt} + d(t) \cdot i_{L1} = d(t) \cdot i_2 + 2d_1(t) \cdot i_2 \\
&L_1 \frac{di_{L1}}{dt} + v_1 = d(t) \cdot v_c \\
&C_1 \frac{dv_1}{dt} + \frac{v_1}{R_1} = i_{L1}
\end{aligned} \tag{13}$$

Next, we simplify the first two equations to the form

$$\begin{aligned}
&L_2 \frac{di_2}{dt} + (1 + d_1(t)) \cdot v_c = v_2 \\
&2C \frac{dv_c}{dt} + d(t) \cdot i_{L1} = (1 + d_1(t)) \cdot i_2
\end{aligned} \tag{14}$$

Now we multiply the first of them by i_2, and the second by v_c, and then add them

$$L_2 i_2 \frac{di_2}{dt} + 2C v_c \frac{dv_c}{dt} + d(t) \cdot i_{L1} v_c = v_2 i_2 \tag{15}$$

We substitute the value $d(t)\cdot v_c$ into the obtained equation and then the current value i_{L1} we substitute from (13)

$$L_2 i_2 \frac{di_2}{dt} + 2Cv_c \frac{dv_c}{dt} + L_1 i_{L1} \frac{di_{L1}}{dt} + C_1 v_1 \frac{dv_1}{dt} + \frac{v_1^2}{R_1} = v_2 i_2 \qquad (16)$$

After the averaging operation of the last equation, we obtain

$$L_2 \tilde{i}_{2.av} \Delta\tilde{i}_2 + 2C\tilde{v}_{c.av}\Delta\tilde{v}_c + L_1 \tilde{i}_{L1.av}\Delta\tilde{i}_{L1} + C_1\tilde{v}_{1.av}\Delta\tilde{v}_1 + \frac{\tilde{v}_{1.av}^2 T}{R_1} = v_2 \tilde{i}_{2.av} T \qquad (17)$$

Considering, as before, that for each period for average values of the load current, $\tilde{i}_{2.av} = \tilde{i}_{1.av} M$, reduced to load voltage current $\tilde{i}_{2.av} = \tilde{i}_{2L} M$, $\Delta\tilde{i}_2 = \Delta\tilde{i}_{2L} M$ and $\tilde{v}_{1.av} = v_2 M$, $M = D/(2-D)$, $\tilde{v}'_{c.av} = D\tilde{v}_{c.av}$ the last equation is written as

$$L_2 M^2 \tilde{i}_{2L}\Delta\tilde{i}_{2L} + \frac{2C}{D^2}\tilde{v}'_{c.av}\Delta\tilde{v}'_c + L_1\tilde{i}_{L1.av}\Delta\tilde{i}_{L1} + C_1\tilde{v}_{1.av}\Delta\tilde{v}_1 + \frac{\tilde{v}_{1.av}^2 T}{R_1} = v_2 i_{1.av} MT \quad (18)$$

and it can match the linear diagram of Fig. 4b ($V = V_2 M$, $L_{eq} = L_1$, $C = C_1$ $R = R_1$), but also having an input filter $L_f - C_f$: $L_f = L_2 M^2$, $C_f = 2C/D^2$. The dynamic mode in it is similar to the dynamic mode of the basic circuit Fig. 4b for averaged values.

5-3. Boost converter with block Up2S. Let us turn to the analysis of the dynamic mode boost converter with the block Up2S (Fig. 5c). Taking as before $i_{La} = i_{Lb} = i_L$ and L_a=L_b=L, we compose a system of equations describing the operation of this circuit:

$$\begin{aligned} &2d(t)\cdot L\frac{di_L}{dt} + 2d_1(t)\cdot L\frac{di_L}{dt} + d_1(t)\cdot v_2 = 2d(t)\cdot v_1 + d_1(t)v_1 \\ &C_2\frac{dv_2}{dt} + \frac{v_2}{R_2} = d_1(t)\cdot i_L \end{aligned} \qquad (19)$$

Now we simplify the first equation to the form

$$2L\frac{di_L}{dt} + d_1(t)\cdot v_2 = (1+d(t))\cdot v_1 \qquad (20)$$

also multiplying it by i_L, and the second equation (19) - by v_2, and then adding them, we get:

$$2Li_L\frac{di_L}{dt} + Cv_2\frac{dv_2}{dt} + \frac{v_2^2}{R_2} = (1+d(t))\cdot v_1 i_L \qquad (21)$$

After the averaging operation of the last equation and, as before, considering that for each period for the averaged values of the currents i_L and i_2 are valid $\tilde{i}_{L.av} = \tilde{i}_{2.av} M1, \Delta\tilde{i}_L = \Delta\tilde{i}_2 M1$, $M1 = 1/(1-D)$ and, $M = (1+D)/(1-D)$, $\tilde{v}_{2.av} = v_1 M$ the last equation is written in the form

$$2LM1^2 \tilde{i}_{2.av} \Delta\tilde{i}_2 + C_2 \tilde{v}_{2.av} \Delta\tilde{v}_2 + \frac{\tilde{v}_{2.av}^2 T}{R_2} = v_1 i_{2.av} MT \qquad (22)$$

The equivalent linear circuit corresponds to this equation - Fig. 4b with parameters:

supply voltage $V = v_1 M$, $L_{eq} = 2LM1^2$, $C = C_2$, $R = R_2$.

5-4. Buck converter with block Dn2D. In conclusion of this section, we consider the circuit diagram of Figs. 1a, 5d with a block Dn2D, in which when feeding in the opposite direction (Fig. 2c), instead of transistors S_a, S_b, of Up2S operate diodes D_a, D_b , and instead of diode D_2, operates transistor S_2). The circuit in general functions as a buck converter with a gain $M = D/(2-D)$.

We compose a system of equations describing the operation of this circuit:

$$\begin{aligned} &2d(t)\cdot L\frac{di_L}{dt} + 2d_1(t)\cdot L\frac{di_L}{dt} + d(t)\cdot v_1 + 2d_1(t)\cdot v_1 = d(t)\cdot v_2 \\ &C_1\frac{dv_1}{dt} + \frac{v_1}{R_1} = d(t)\cdot i_L + 2d_1(t)\cdot i_L \end{aligned} \qquad (23)$$

Simplifying these equations to the form

$$\begin{aligned} &2L\frac{di_L}{dt} + (1+d_1(t))\cdot v_1 = d(t)\cdot v_2 \\ &C_1\frac{dv_1}{dt} + \frac{v_1}{R_1} = (1+d_1(t))\cdot i_L \end{aligned} \qquad (24)$$

and multiplying the first equation by i_L, and the second equation by v_1, and then adding them we get:

$$2Li_L\frac{di_L}{dt} + Cv_1\frac{dv_1}{dt} + \frac{v_1^2}{R_1} = d(t)\cdot v_2 i_L \qquad (25)$$

After the averaging operation of the last equation and, as before, considering that for each period for average values $\tilde{i}_{L.av} = \tilde{i}_{1.av} M1$, $M1 = 1/(2-D)$ and, $\tilde{v}_{1.av} = v_2 M$, $M = D/(2-D)$ the last equation is written in the form

$$2LM1^2\tilde{i}_{1.av}\Delta\tilde{i}_1 + C_1\tilde{v}_{1.av}\Delta\tilde{v}_1 + \frac{\tilde{v}_{1.av}^2 T}{R_1} = v_2 i_{1.av} MT \qquad (26)$$

The equivalent linear circuit Fig. 4,b $L_{eq} - (C \| R)$, corresponding to this equation will have the parameters: $V = v_2 M$ и $L_{eq} = 2LM1^2$, $C = C_1$, $R = R_1$.

6. Formation of equivalent conventional converters

6-1. Boost converter with block Up1D. In this section, we will try, to receive the scheme of equivalent boost or buck converters based on the obtained equations and structures of the equivalent linear circuit. Indeed, in order to conversion from a linear circuit back to a boost converter circuit, it is necessary to use inductance $L = L_{eq}(1-D)^2$ and supply voltage $V = V_{in}(1+D)$ in this converter, leaving the parameters *C* and *R* unchanged.

Following this principle, for the equivalent linear circuit obtained for boost converter with Up1D link, the conventional boost converter will have the following parameters $V = V_{in}(1+D)$, $C = (C_{eq} + C_2)$, $R = R_2$, $L_{eq} = (L_{1.eq} + L_{2.eq})(1-D)^2$.

The dynamic characteristics of the resulting converter are completely identical to the more complex initial boost converter circuit with the Up1D cell and, which is especially important, both when the supply voltage changes, and when the duty cycle changes. Fig. 6a shows the results of testing the proposed methodology in the PSPICE program using the example of boost converter with the Up1D cell and with parameters: $L_1=600\mu H$, $L_2=1000\mu H$, $C=0.5\mu F$, $C_2=0.2\mu F$, $R_2=200\Omega$ first when turned on $V_{in}=12V$ at $D=0.5$, and then with a drastic change in duty cycle to $D=0.75$.

6-2. Buck converter with block Dn1S. Next, we compare the conventional buck converter, which would be equivalent to the original buck converter with the Dn1S. We will be based on the previously obtained linear circuit, from which it is easy to obtain the structure of a conventional buck converter - input voltage $V = V_{in}M1$, $M1 = 1/(2-D)$, then the input *L-C* filter – $L_f=L_2M1^2$, $C_f = 2C$, and then buck converter with output inductance $L = L1$, output capacitance $C = C1$ and load $R = R1$. Fig. 6b, shows the results of testing the proposed methodology in the PSPICE program are shown using the buck converter example with block Dn1S and with block Up1D parameters and at $V2 = 36V$, $R1 = 8$ Ohm. Fig. 6b shows the

curves of the output current i_{L1}, as well as the output voltage v_o in the initial and equivalent buck converter. Initially, both converters are turned on at $D = 0.5$, and then with a sudden change in duty cycle to $D = 0.75$. The test results show a good agreement between the obtained voltage and current curves.

6-3. Boost converter with block Up2S. The dynamic characteristics in the case of the initial boost converter circuit with block Up2S are completely identical to the dynamic characteristics of the conventional boost converter with an input inductance of *2L* and a supply voltage $V = V_{in}(1+D)$. Parameters *C2* and *R2* remain unchanged. As in previous cases, the identity is remained both when the supply voltage changes, and when the duty cycle changes. In Fig. 6c shows the results of testing the proposed methodology in the PSPICE program using the boost converter as an example with block Up2S and with parameters: $L1=400\mu H$, $C2=5\mu F$, $R2=50\Omega$ at the beginning when turning on the voltage $Vin=12V$ at $D=0.5$, and then with a drastic change of the duty cycle to $D=0.75$.

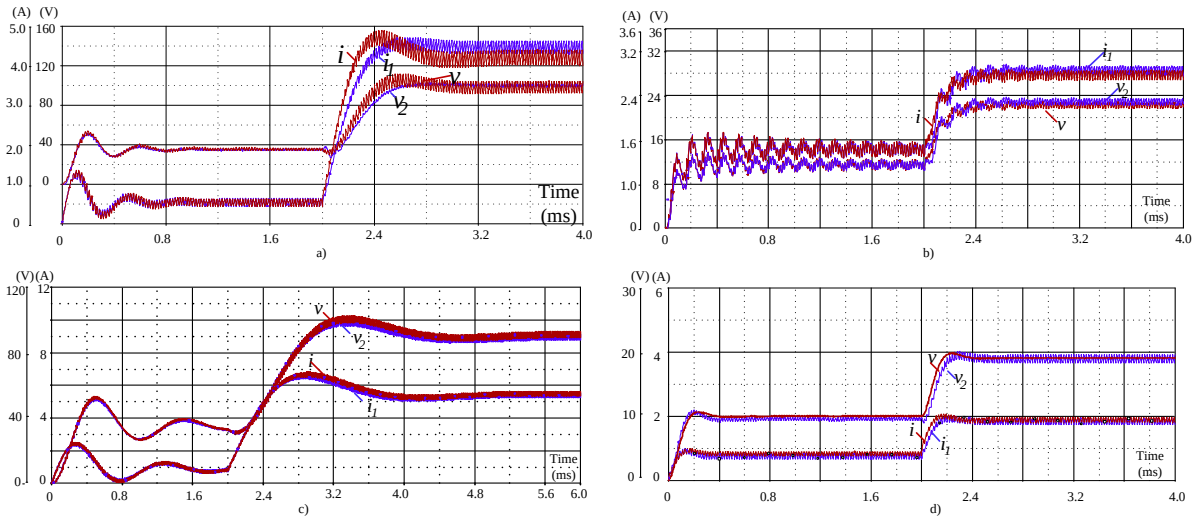

Fig. 6: An example of the process of turning on different converters with a different links and its equivalent converter for constant voltage at *D = 0.5* with subsequent change at *t = 2ms* duty cycle to D = 0.75 (a) boost converter with an Up1D link (b) buck converter with a Dn1S link (c) boost converter with an Up2S link (d) buck converter with a Dn2D link.

6-4: Buck converter with block Dn2D. Similarly, for a buck converter with block Dn2D in the equivalent conventional buck converter circuit, the input voltage $V = V_{in}/(1+D_1)$ and inductance will be *L*. The results of testing the proposed method in the PSPICE program using the buck converter with a Dn2D link with parameters: $V2=36V$, $L1=600\mu H$, $C1=6\mu F$,

R1=8Ω. are presented in Fig. 6d. It shows the curves of the output voltage and output current of the initial and equivalent conventional buck converter - first, when turned on, the voltage is at *D=0.5*, and then when the duty cycle changes abruptly to *D=0.75*.The test results show a good agreement between the obtained voltage and current curves. In all graphs Fig. 6 the values of currents in the original and equivalent converters are reduced to one value.

In conclusion, we note that converters with Up3D, Dn3S links, as can be easily see, will correspond to linear equivalent circuits that coincide with the circuits for converters with Up2S, Dn2D. Similarly, we get the same coincidence for pairs of blocks - Dn1D and Dn1S, Up1S and Up1D.

The remaining four blocks - Dn3D, Up3S and Up2D, Dn2S are not considered here, since their use is associated with buck-boost, Cuk, Sepic and Zeta converters and requires a significant increase in the size of the paper.

7. EXPERIMENT RESULTS

An experimental verification of the obtained theoretical results of the transients analysis was performed for the Dn2D-Up2S converter (Figs. 7 and 8).

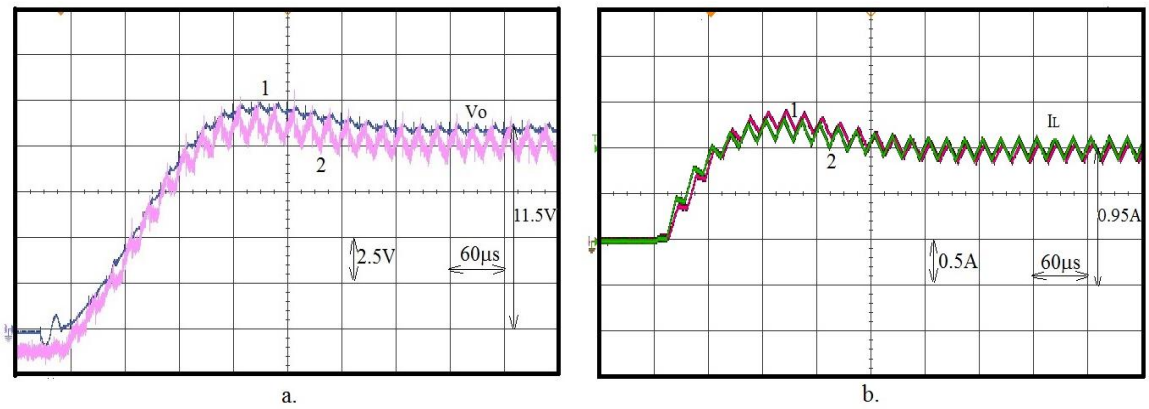

Fig. 7: The process of turning on buck converter with a block Dn2D – (1) and its equivalent converter – (2) for constant voltage at D = 0.5 (a) - output voltages (b) – inductor currents.

The parameters of the laboratory model were as follows: *Vin=36V, L1 = L2 = 600µH, C = 6µF, R = 8Ω, f = 50 kHz, D = 0.5*. The parameters of the conventional buck converter, providing the same dynamic characteristics as the original converter Dn2D, according to paragraph 6-4 were *Vin=24V, L= 600µH*, and the other parameters remained unchanged.

Fig. 8 shows the curves of the output voltage (Fig. 8a) and inductance current (Fig. 8b) during the starting the two above converters - converter Dn2D and convectional buck convertor, at a constant voltage. The corresponding curves in both cases practically coincide.

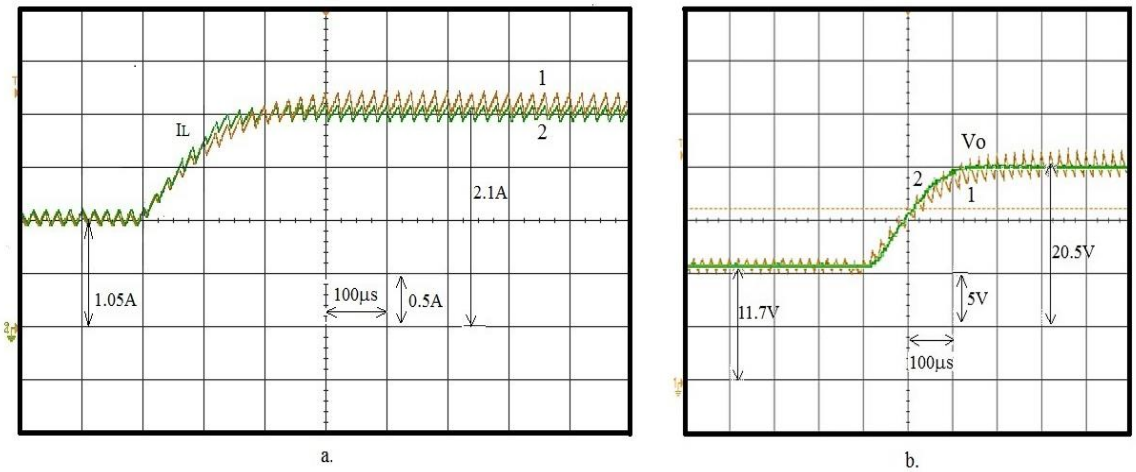

Fig. 8: The process with an abrupt change in the duty cycle from D = 0.5 to D= 0.75 on buck converter with a link Dn2D (1) and its equivalent converter (2); (a) – currents, (b)– voltages.

Similarly, Fig. 8 shows the curves of the output voltage and inductance current with an abrupt change in the duty cycle from $D = 0.5$ to $D = 0.75$ with $R = 8\Omega$. Moreover, Fig. 8 displays the transient in converter Dn2D – curve 1, and in the conventional buck convertor - curve *2*. In the second case, the supply voltage also changed simultaneously with the duty cycle: at $D = 0.5$, $Vin=24V$, and at $D = 0.75$ $Vin = 28.8V$. In Fig. 8a current *2* is reduced to current *1* using the multiplier $1/(2-D)$. And in this case, the processes in two types of converters - basic and equivalent, proceed are completely identically. It should be emphasized that the inductance value of the equivalent conventional converter remains unchanged when the duty cycle changes.

8. CONCLUSIONS

1. The use of bidirectional switches in the switching-capacitor and switching-inductor structures instead of diodes allows you to expand their functions, providing with the same type of structure both the possibility of increasing the output voltage and decreasing it.
2. The modules with bidirectional switches allow creating a wide family of bidirectional converters based on classic DC-DC converters with an extended range of output voltage regulation in each direction.

3. To analyze the dynamics of such converters having a rather complicated structure, a methodology for replacing them with an equivalent circuit of a conventional converter of the same type, the dynamic characteristics of which are well known, is proposed.

REFERENCES

1. Axelrod, B., Berkovich, Y., Ioinovici, A., "Transformerless DC-DC converters with a very high DC line-to-load voltage ratio", Circuits and Systems 2003, ISCAS‘03, Proc. 2003 Int’l. Symp. on Circuits and Systems (ISCAS 2003), Bangkok, Thailand, May 2003; III: 435-438, 25-28.
2. Axelrod, B., Berkovich, Y., Ioinovici, A. (2004), "Transformerless dc-dc converters with a very high dc line-to-load voltage ratio", J. Circuits, Systems and Computers, 2004; 13(3): 467-475.
3. Axelrod, B., Ioinovici, A., Berkovich, Y. (2004), "Single-switch single-stage switched-capacitor buck converter", 4th Nordic Workshop on Power and Ind. Electron. (NORPIE 2004), Trondheim, Norway, June 2004; 14-16.
4. Axelrod, B., Berkovich, Y., Ioinovici, A. (2006) 'Switched-Capacitor (SC)/switched inductor (SL) structures for getting hybrid step-down Ćuk/Sepic/Zeta converters', Proc. IEEE Int'l. Symp. on Circuits and Systems (ISCAS '2006), Kos, Greece, May 2006; 5063-5066, 21-24.
5. Axelrod, B., Berkovich, Y., Ioinovici, A. (2008), "Switched-capacitor/switched-inductor structures for getting transformerless hybrid DC-DC PWM converters", *IEEE Trans. on Circuits and Systems I*, 2008; 55(2): 687-696.
6. Axelrod, B., Berkovich, Y., Tapuchi, S., *et al*. (2009), "Single-stage single-switch switched-capacitor buck/buck-boost-type converter", IEEE *Trans. on Aerospace and Electron. Systems*, 2009; 45(2): 419-430.
7. Axelrod, B., Berkovich, Y., Ioinovici, A. (2006), "Switched coupled-inductor cell for DC-DC converters with very large conversion ratio", The 32nd Annual Conf. IEEE Ind. Electron. Society (IECON’06), Paris, France, Nov. 2006; 2366-2371, 7-10.
8. Axelrod, B., Berkovich, Y., Tapuchi, S., *et al*. (2009), "Improved circuit of the switched coupled-inductor cell for dc-dc converters with very large conversion ratio", Proc. 13th European Conf. on Power Electron. and Applications (EPE 2009), Barcelona, Spain, September, 2009; 8-10.

9. Axelrod, B., Berkovich, Y., Shenkman, A., *et. al*. (2012), "Diode-capacitor voltage multipliers combined with boost-converters: Topologies and characteristics", *IET Power Electron.*, 2012; 5(6): 873-884.
10. Axelrod B., Berkovich Y., and Beck Y. (2019), "A Family of Universal Bidirectional DC-DC Converters with Extended Voltage Gain", *IET Power Electron*., 2019; 12(13): 3562-3570.
11. Axelrod, B., Beck, Y., Berkovich, Y. (2015), "High step-up DC-DC converter based on the switched-coupled-inductor boost converter and diode-capacitor multiplier: Steady state and dynamics", *IET Power Electron.*, 2015; 8(8): 1420-1428.
12. Amir, A., Amir, A., Che, H., S., *et al.* (2018), "Comparative Analysis of High Voltage Gain DC-DC Converter Topologies for Photovoltaic Systems", Int. J. Renewable Energy, September 2018; 1-35.
13. Baek J. W., Ryoo M. H., Kim T. J., *et al.* (2005), "High boost converter using voltage multiplier", Proc. IEEE Ind. Electron. Conf., Raleigh, USA, November, 2005; 6-10.
14. Cornea O., Andreescu G-D., Muntean N., *et al*. (2017), "Bidirectional Power Flow Control in a DC Microgrid through a Switched-Capacitor Cell Hybrid DC-DC Converter", *IEEE Trans. on Ind. Electron.*, 2017; 64(4): 3012 – 3022.
15. Chung-Ming Young, Ming-Hui Chen, Tsun-An Chang, *et al.*, "Cascade Cockcroft–Walton Voltage Multiplier Applied to Transformerless High Step-Up DC–DC Converter", *IEEE Trans. on Ind. Electron.*, 2013; 60(2): 523-537.
16. De Paula, A., N., De Castro Pereira, D., De Paula, W., J., *et al*. (2014), "An Extensive Review of Nonisolated DC-DC Boost-Based Converters", IEEE Conf. Paper, December, 2014; 1-10.
17. Fei Li, Yu Yao, Zhi Wang, *et al*. (2018), 'Coupled-inductor-inverse high step-up Converter', *IET Power Electron.*, 2018; 11(5): 902-911.
18. Feng P., and Tapan S. (2006), "Charge pump circuit design", (McGraw-Hill, 2006).
19. Forouzesh, M., Siwakoti, Y., Gorji, S., *et al*. (2017), "Step-Up DC–DC Converters: A Comprehensive Review of Voltage-Boosting Techniques, Topologies, and Applications", *IEEE Trans. on Power Electron.*, December, 2017; 32(12): 9143-9178.
20. Girish Ganesan, R., Prabhakar, M. (2013), "Non-Isolated High Gain Boost Converter for Photovoltaic Applications", Int. Conf. on Power, Energy and Control (ICPEC), 2013; 273-280.

21. Girish Ganesan, R., Prabhakar M. (2014), "A novel interleaved boost converter with voltage multiplier cell", IEEE 2nd Int. Conf. on Electrical Energy Systems (ICEES), 2014; 183-188.
22. Ioinovici, A. (2013), "Power Electronics and Energy Conversion Systems, Fundamentals and Hard-switching Converters, 2013; (1)" (Wiley, 2013), 868.
23. Ioinovici, A. (2001), "Switched-capacitor power electronics circuits", *IEEE Circuits Syst. Mag.*, 2001; 1(3): 37–42.
24. Li, K., Hu, Y., and Ioinovici, A. (2016), "Generation of the Large DC Gain Step-Up Non-Isolated Converters in Conjunction with Renewable Energy Sources Starting from a Proposed Geometric Structure", *IEEE Trans. on Power Electron*., Sept. 2016.
25. Liang, T-J., Chen, S-M., Yang, L-S., *et al*. (2012),"Ultra-Large Gain Step-Up Switched-Capacitor DC-DC Converter With Coupled Inductor for Alternative Sources of Energy", *IEEE Trans. on Circuits and Systems I: Regular Papers*, April 2012; 59(4): 864-874.
26. Li-Jun, J., Guang-Yao, Y., Miao-Miao, J., *et al*. (2015), "Study of bi-directional DC-DC converter of micro-grid hybrid energy storage system", *IEEE 10th Conf. on Ind. Electron. and Appl., (ICIEA)*, Auckland, 2015; 1166-1169.
27. Luo, F. L.; Hong, Y. "Hybrid split capacitors and split inductors applied in positive output super-lift Luo-converters", *IET Power Electronics*, 6(9): 1759-1768.
28. Luo, F. L. (2011), "Investigation on hybrid Split-Capacitors and Split-Inductors applied in Positive Output Super-Lift Luo-Converters", Proc. Ind. Electron. and Applications, June, 2011; 328-334.
29. Maksimovic´, D., C´uk, S. (1991), "Switching converters with wide DC conversion range", IEEE Trans. Power Electron., 1991; 6(1): 151–157.
30. Middlebrook R. D., and Ćuk, S. (1976), "A general Unified Approach to Modeling Switching-Converter Power Stages", IEEE PESC, 1976.
31. Pathak, A., Sahu, V. (2015), "Review & Study of Bidirectional of DC-DC Converter Topologies for Electric Vehicle Application", Int. Journal of Science, Engineering and Technology, 2015; 3: 6.
32. Prince, R., Kalaivani, R. (2013), "DC-DC Converter Based on Cascade Cockcroft-Walton Voltage Multiplier for High Voltage Gain without Using Transformer", Int. Journal of Engineering Science and Innovative Technology (IJESIT), March, 2013; 2(2): 464-474.

33. Pyosoo Kim, Sanghyuk Lee, Junsung Park and *et al*. (2011), "High Step-up Interleaved Boost Converters Using Voltage Multiplier Cells", 8th Int. Conf. on Power Electron., ECCE Asia, The Shilla Jeju, Korea, 2011; 2844-2851.
34. Rong-Jong Wai**,** Chung-You Lin, Rou-Yong Duan, *et al*. (2007), "High Efficiency DC-DC ConverterWith High Voltage Gain and Reduced Switch Stress", *IEEE Trans. on Ind. Electron*., February, 2007; 54(1): 354-364.
35. Sivakumar, S., Sathik, M., J., Manoj, P., S., *et al*. (2016), "An assessment on performance of DC–DC converters for renewable energy applications", Renewable and Sustainable Energy Reviews, 2016; 58: 1475–1485.
36. Yanying Gao, Hongchen Liu, and Jian Ai. (2018), "Novel High Step-Up DC–DC Converter with Three-Winding-Coupled-Inductors and its Derivatives for a Distributed Generation System", Energies, 2018; 11: 3428: 2-12.
37. Zhao, Q., Lee, F.C. (2003), 'High-efficiency, high step-up DC–DC converters', IEEE Trans. Power Electron., 2003; 18(1): 65–73.
38. Zhao, Q., Tao, F., Lee, F. C. (2001), "A front-end DC/DC converter for network server applications", Proc. IEEE – PESC, 2001; 1535–1539.
39. Wai, R.-J., Duan, R.-Y. (2005), 'High step-up converter with coupled inductor', *IEEE Trans. Power Electron*., 2005; 20(5): 1025–1035.